JBC RESEARCH ARTICLE

AMH regulates a mosaic population of AMHR2-positive cells in the ovarian surface epithelium

Received for publication, February 12, 2024, and in revised form, October 7, 2024 Published, Papers in Press, October 17, 2024,
https://doi.org/10.1016/j.jbc.2024.107897

Elizabeth R. Smith[1], **Dorcus Ye**[2], **Shihua Luo**[3], **Isaac R. L. Xu**[4], **and Xiang-Xi Xu**[2,3,*]

From the [1]*Department of Obstetrics, Gynecology and Reproductive Sciences, University of Miami Miller School of Medicine, Miami, Florida, USA;* [2]*Sylvester Comprehensive Cancer Center, University of Miami Miller School of Medicine, Miami, Florida, USA;* [3]*Department of Radiation Oncology, University of Miami Miller School of Medicine, Miami, Florida, USA;* [4]*Dr. John T. Macdonald Foundation, Department of Human Genetics and John P. Hussman Institute for Human Genomics, University of Miami Miller School of Medicine, Miami, Florida, USA*

Reviewed by members of the JBC Editorial Board. Edited by Paul Shapiro

The function and homeostasis of the mammalian ovary depend on complex paracrine interactions between multiple cell types. Using primary mouse tissues and isolated cells, we showed *in vitro* that ovarian follicles secrete factor(s) that suppresses the growth of ovarian epithelial cells in culture. Most of the growth suppressive activity was accounted for by Anti-Mullerian Hormone/Mullerian Inhibitory Substance (AMH/MIS) secreted by granulosa cells of the follicles, as determined by immune depletion experiments. Additionally, conditioned medium from granulosa cells from wild-type control, but not AMH knockout, suppressed epithelial cell growth. Tracing of the AMH-regulated cells using AMHR2 (AMH receptor 2)-Cre:ROSA26 mutant mice indicated the presence of populations of AMHR2-positive epithelial cells on the ovarian surface and oviduct epithelia. Cells isolated from the mutant mice indicated that a subpopulation of cells marked by AMHR2-Cre:ROSA26 accounted for most cell growth and expansion in ovarian surface epithelial cells, and the AMHR2 lineage-derived cells were regulated by AMH *in vitro*; whereas, fewer AMHR2-Cre:ROSA26-marked cells accounted for oviduct epithelial cell outgrowth. The results reveal a paracrine pathway in maintaining follicle-epithelial homeostasis in the ovary and support a subpopulation of AMHR2 lineage marked epithelial cells as ovarian epithelial stem/progenitor cells with higher proliferative potential regulatable by follicle-secreted AMH.

Complex paracrine interactions between multiple cell types contribute to maintaining the tissue function, structure, and homeostasis of the mammalian ovary (1, 2). Oocyte growth and differentiation depend upon the coordinated development of the follicle and its increasing numbers and specialization of granulosa cells to provide regulatory and nutritional signals to the oocyte (3, 4), and oocytes in turn regulate the crucial progression of follicle development, promoting granulosa cell proliferation and differentiation in primary and antral follicle formation (5). Communication between granulosa cells and the theca cells that surround the periphery of a follicle stimulates antral follicle formation (6). The ovarian surface epithelium must also repair the site that ruptured during ovulation of the primary dominant follicle (7). Ovulation is initiated in response to a surge of pituitary gonadotropins and granulosa-derived cyclooxygenase enzymes, followed by localized apoptosis of ovarian surface epithelial cells. Presumably, a progenitor cell population replicates and migrates to cover the wound site, and the process repeats cycle dependently throughout a female's reproductive lifespan.

The depletion of ovarian follicles later in the reproductive lifespan results in menopause in women. Although the post-reproductive lifespan is especially long in humans, most animals, including laboratory models, undergo reproductive senescence (8, 9), though the loss of oocytes to atresia is principally responsible for menopause in humans. The ovarian tissue structure then undergoes substantial changes as the balance between the various ovarian cell types is disrupted (9, 10). Among the consequences of depletion of ovarian follicles and germ cells, the ovarian surface and oviduct epithelial cells undergo morphological aging (11), where the surface epithelium thickens and becomes irregular (10). In the White Spotting Variant Wv/Wv mice that have a c-kit mutation and reduced germ cells and follicles (12–14), and which we previously characterized as a mouse model of menopause (15), the ovarian surface epithelial cells proliferate intensely and form tubular adenomas, a benign tumor that infiltrates into the ovary (16, 17). Deletion of either Tp53 or cyclooxygenase 1 (Cox1) reduces epithelial lesions in the WvWv mice, which can be attributed to the persistence of ovarian follicles in the compound mutant mice (18, 19). Cox2 heterozygous deletion in the Wv/Wv mice also reduces epithelial tumor development, suggesting Cox2 inflammatory signaling is involved in stimulating epithelial growth (20); however, homozygous deletion of Cox2 has no protective effect, due to increased Cox1 expression that compensates for the loss of Cox2 in the Cox2 (−/−) mice. In general, we observed a strict inverse correlation between epithelial lesions and the presence of granulosa cells (21). These earlier studies indicate a critical

* For correspondence: Xiang-Xi Xu, xxu2@med.miami.edu.
Present address for Dorcus Ye: Department of Obstetrics and Gynecology, Burin Peninsula Healthcare Centre, Newfoundland, Canada.

role of ovarian follicles in regulating the homeostasis of ovarian epithelial cells.

To understand how the microenvironment affects the regulation of the ovarian surface epithelium, as well as perhaps other localized epithelia such as the fallopian tube fimbria, we investigated Anti-Müllerian Hormone/Müllerian Inhibitory Substance (AMH/MIS) secreted by granulosa cells of ovarian follicles. The receptor for the hormone or autocrine factor is AMHR2/MISR2 (Anti-Müllerian Hormone Receptor type 2/ Müllerian Inhibitory Substance Receptor Type 2), which is generally considered expressed in the stroma of female reproductive tissues, rather than epithelial cells (19, 22–24). However, in AMHR2-cre;ROSA26 reporter mice, AMHR2-positive epithelial cells are also detected in a mosaic expression pattern in both ovarian surface and oviduct epithelia (21). Possibly, ovarian follicle-derived AMH may suppress epithelial growth either through stromal interactions and control or by directly impacting the AMHR2-positive epithelial population. Using primary mouse tissues and isolated cells, we found a subpopulation of ovarian surface epithelial cells marked by AMHR2 lineage with proliferative potential and responsive to follicle-secreted AMH. Thus, the decline in AMH levels with menopause may contribute to a permissive environment for some ovarian tumor development, but other important factors must be involved.

Results

Co-culture with granulosa cells and conditioned medium suppresses epithelial cell growth

Repeated experiments show that isolated mouse ovarian surface epithelial (MOSE) cells proliferate under normal culture conditions. In contrast, primary oviduct (OVD) epithelial cells can be isolated and maintained but do not appear to proliferate as readily or consistently under the same conditions (Fig. 1, *A* and *B*), as reported by others for human fallopian tube epithelial cells (25, 26). MOSE cells exhibited a differential response to being co-cultured in the presence of granulosa cells (Fig. 1*C*). Here, MOSE cells were plated in a transwell system on the bottom of tissue culture dishes in which granulosa cells were grown on filters suspended in the same well, where the medium was shared between the two cell types. Co-culture with granulosa cells reduced MOSE cell proliferation 6% after 2 days and 30% after 4 days (Fig. 1*C*).

Since the granulosa cells do not physically touch the MOSE cells in the transwell co-cultures, the results suggest that the granulosa cells likely secrete a factor that inhibits MOSE proliferation. We then monitored MOSE cell growth in the presence of a conditioned medium collected from cultures of isolated mouse granulosa cells obtained from females stimulated according to the PMS/hCG protocol (27, 28). Conditioned medium (GCCM) was prepared from granulosa cells after culture for 2 (2 days) or 4 (4 days) days and added to MOSE cultures for 4 days. The proliferation of MOSE cells was sensitive to both the concentration of granulosa cell-conditioned culture medium and the period of conditioning, where the relative cell number was reduced by approximately 50% in cultures incubated with 50% granulosa cell-conditioned medium. Cell numbers were further reduced by approximately 67% in 80% granulosa cell conditioned medium obtained from 4-day cultures compared to 2-day cultures (Fig. 1*D*). As a control, we also isolated granulosa cells using DES priming of the mice (29), which mostly captures tertiary and early antral follicles, and found similar effects of granulosa cell-conditioned medium on MOSE proliferation (Fig. S1). This suggested that isolated granulosa cells behaved similarly in the experimental culture conditions regardless of the priming protocol, and we subsequently used the more common hCG protocol for all subsequent assays. MOSE cells grown in the presence of granulosa cells were compromised, showing obvious signs of decline (Fig. 1*E*).

Granulosa cell AMH suppresses ovarian surface and oviduct epithelial cell growth in vitro

Granulosa cells produce and secrete growth factors, hormones, and other active factors to support and maintain oocyte maturation, ovulation, and pregnancy. One significant granulosa-derived candidate that might regulate epithelial activity is AMH, a member of the TGFβ superfamily of signaling molecules. AMH is produced in greatest amounts by small and medium antral follicles (6), although it is expected to still be expressed in granulosa cells just prior to luteinization (30), and negatively regulates follicle recruitment at the transition from primordial to primary follicle stage and inhibits FSH-dependent cyclical recruitment of follicles (31). AMH, like other TGFβ family members, is synthesized from a dimeric precursor consisting of a large N-terminal prodomain and an active C-terminal signaling domain and undergoes processing to cleave the signal sequence (32). Only the cleaved, processed dimer form properly binds to its receptors and induces downstream signaling (32–34).

We treated primary MOSE cells with a commercially available AMH (R&D Systems) that appears to consist principally of an approximately 12 kDa protein that represents the C-terminal end of AMH/MIS, which is thought to contain the bioactivity of the protein. TGFβ suppressed MOSE proliferation by 36% (Fig. 2*A*), yet while the suppressive effect was significant, AM did not reduce MOSE proliferation to the same extent TGFβHowever, both AMH and TGFβ treatment consistently resulted in similar morphological effects on MOSE cell cultures, where cells appeared patchy, raised, and lacking the clear, confluent lawn of cuboidal epithelial cells found in control cultures (Fig. 2*B*). These results are perplexing, though may relate to variable commercial AMH stability and bioactivity, which have been reported to be sensitive to purification methods and reconstitution (2, 35, 36).

These observations prompted us to investigate whether AMH present in our *in vivo* culture system might suppress the proliferation of normal wild-type MOSE cells. Indeed, when we immunodepleted AMH from granulosa cell conditioned medium using an excess concentration of an anti-AMH rabbit polyclonal antibody that recognizes mouse AMH (abcam ab84952), MOSE cell growth was nearly 75% control (no

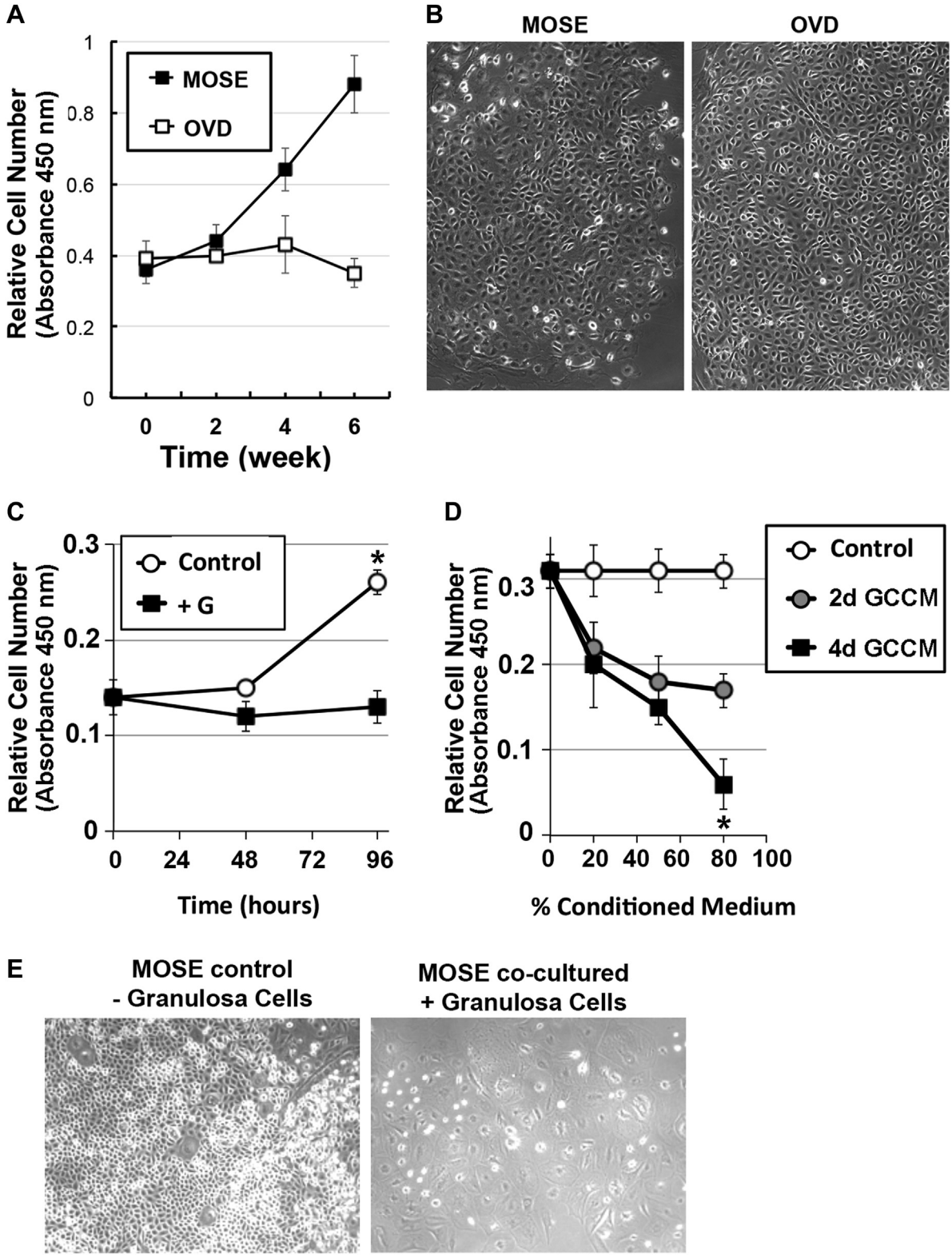

Figure 1. Granulosa factor(s) suppress MOSE cell growth in culture. *A*, primary MOSE and OVD cells were isolated from wild-type mice and expanded in culture. Proliferation of cells was determined using a WST-1 assay, where cell number correlates with the absorbance measured at 450 nm. Relative cell numbers were measured in triplicate samples and are represented as the mean ± s.d. *B*, both MOSE and OVD have a characteristic cuboidal epithelial shape in culture. *C*, MOSE cells were co-cultured in transwell dishes with (+G) or without (control) granulosa cells (+G). Cell number was determined by the WST-1 proliferation assay kit. *D*, Conditioned medium was prepared from granulosa cells after 2 (2 days) or 4 (4 days) days in culture. MOSE cells were plated in triplicate in 96-well dishes and grown overnight, then incubated in granulosa cell conditioned medium (GCCM) mixed with normal culture medium at the percentages shown; cell number was assayed after 4 days in culture, when MOSE cells are actively proliferating. Data are expressed as mean ± s.d., with $*p < 0.05$, by Student's unpaired two-tailed *t* test. *E*, representative images of MOSE cells co-cultured without (Control) or with (+Granulosa) granulosa cells.

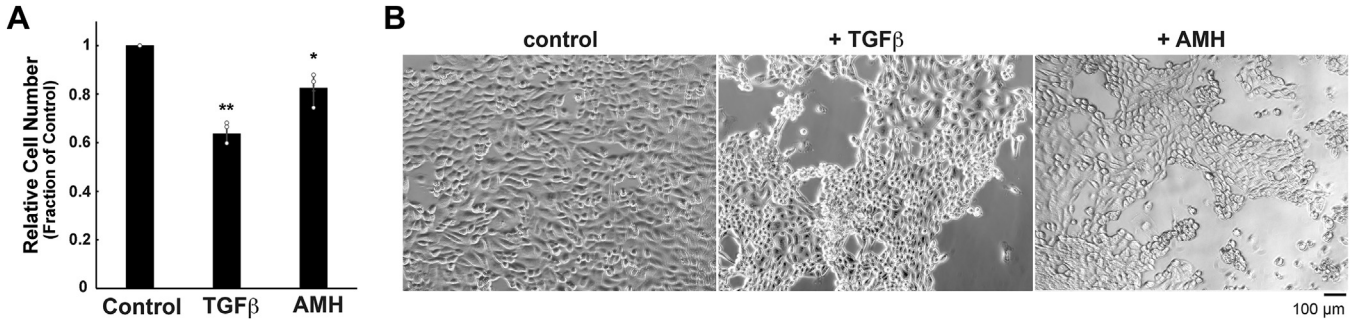

Figure 2. AMH suppresses MOSE cell growth. *A*, MOSE cells were treated with TGF-β (0.1 μg/ml) or AMH (5 μg/ml) for 4 days, and cell growth was determined by WST-1 assay and expressed as the cell number of treated cells relative to control cells (fraction of control). The average of three experiments is shown as mean ± s.d., with $*p < 0.05$ or $**p = 0.001$, determined by an unpaired two-tailed Student's *t* test. *B*, images of cells treated with TGF-β or AMH, as described.

GCCM) (Fig. 3*A*). Untreated GCCM exerted remarkable ≈60% suppression compared to control and ≈55% suppression relative to anti-AMH. Moreover, MOSE cells grown in the presence of wild-type granulosa cell conditioned medium proliferated ≈50% less than cells cultured in the presence of granulosa cell conditioned medium isolated from AMH knockout females (Fig. 3*B*). AMH knockout and wild-type mice and granulosa cell cultures were age-matched and treated identically. These combined results establish that AMH contributes significantly to suppressing epithelial cell growth in culture.

AMH signals *via* a dimeric type I and dimeric type II serine/threonine receptor kinases, and is unique among the TGFβ family as its type II receptor AMHR2 is solely specific for

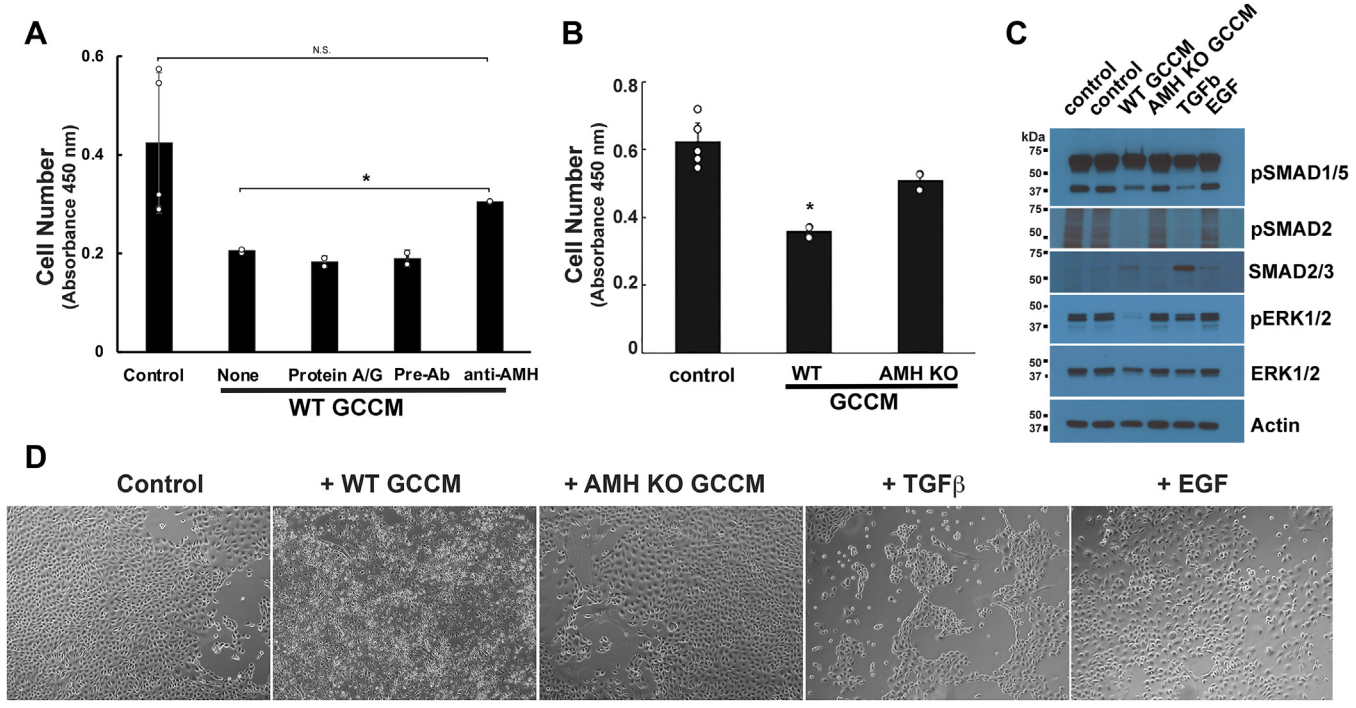

Figure 3. AMH from granulosa cell conditioned medium suppresses MOSE growth in culture. *A*, AMH was immunodepleted from granulosa cell conditioned medium (GCCM) using an excess concentration of anti-AMH rabbit polyclonal antibody (Abcam ab84952) (Anti-AMH). Controls included normal culture medium (control) and granulosa cell conditioned medium that had no treatment (none), treated only with the affinity matrix used for IP (+ protein A/G), or non-specific pre-immune rabbit serum and Protein A/G (Pre-Ab). MOSE cultures were treated with the respective medium for 6 days, and relative cell number was determined by WST-1 assay, shown as mean ± s.d., with $*p < 0.05$, as determined by an unpaired two-tailed Student's *t* test. The error bars indicate multiple and potentially overlapping measurements. There was no significant difference (N.S.) between cell proliferation in control medium and anti-AMH immunodepleted granulosa cell conditioned medium; however, a significant difference was determined between cells grown in untreated granulosa cell conditioned medium (none) and anti-AMH immunodepleted granulosa cell conditioned medium. *B*, granulosa cells were isolated from wild-type or AMH knockout mice and grown in culture for 6 days. The conditioned medium was collected and incubated with MOSE cells for an additional 6 days. The effect of granulosa cell conditioned medium from normal wild type or AMH knockout mouse ovaries was compared to normal culture medium. MOSE cell proliferation was significantly decreased by growth in WT GCCM, determined as $*p < 0.05$ by an unpaired two-tailed Student's *t* test. *C*, MOSE cells were treated with TGFβ, EGF, or granulosa cell conditioned medium for 6 days, then collected in sample buffer, and analyzed by Western blot for the proteins indicated. *D*, images of cells treated with TGFβ, EGF, and conditioned medium collected from wild type (WT) or AMH KO granulosa cells grown in culture for 6 days.

AMH and does not bind other family members (32). AMH binding to its cognate receptor AMHR2 triggers conjugation to its type I receptor to commence canonical signaling through SMADs (33). Both AMH and TGFβ upregulated SMAD2/3 levels and reduced phospho-SMAD2 and phospho-SMAD1/5, and lowered phospho-ERK1/2 levels, as compared to other treatments (Fig. 3*C*). As predicted, MOSE cells cultured in the presence of WT GCCM showed clear signs of cell death, which was not found in AMH knockout GCCM (Fig. 3*D*).

AMHR2 lineage cells of the ovarian surface and oviduct have increased capacity for proliferation

We traced AMHR2 expression in cells *in vitro* and *in vivo* to examine where AMH might target epithelial growth, since AMHR2 is required for AMH to initiate signaling, it should also be present in the targeted tissue or cells (37). Shown in Fig. 4, *A* and *B*, lineage tracing of AMHR2 expression using the AMHR2-Cre+; Rosa26 ± breeding and XGal staining for β-galactosidase (LacZ) confirm variable heterogeneous AMHR2 expression in the ovarian surface and oviduct epithelium and more consistent staining in the granulosa cells of ovarian follicles and the uterine epithelium. Moreover, when the AMHR2-Cre+; Rosa26 ± mice were crossed onto the Wv background, AMHR2-mediated LacZ staining predominated in the hyperproliferative areas of the benign tumors of the WvWv homozygous ovaries (Fig. 4*C*). These data suggest that AMHR2-labeled cells have the capacity for proliferation and expansion and constitute most of the tubular adenomas that develop.

To understand if AMHR2-positive epithelial cells can mark a stem cell population and potential precursor/proliferative population, we isolated wild-type normal and AMHR2-Cre+;ROSA26 ± ovarian surface and oviduct epithelial cells and monitored the outgrowth of cells over a 4-weeks time course (Figs. 5, S2). XGal-stained, LacZ-positive cells expanded rapidly in MOSE cultures, from ≈10% when first plated (week 0), to ≈80% by week 4 (Fig. 5, *A* and *B*). All cells expanded over the course of the experiment but AMHR2+ cells (shown as XGal+) outgrew the normal wild type cells. These isolated MOSE cells were responsive to EGF, as well as stem cell growth factors LIF and β-ME (Fig. S3), that over the time course of expansion likely selected stem-like cells marked by AMHR2. In contrast, LacZ-positive oviduct epithelial cells were rarer and increased more slowly, such that they were only clearly discernible after 4 weeks, when ≈17% were stained with X-Gal (Fig. 5, *C* and *D*). This might be predicted based on their general growth properties in culture. However, AMHR2-negative cells expanded in culture; these cells did not exhibit spurious LacZ staining that might be attributed to senescence-induced lysosomal β-galactosidase expression (38).

In the AMHR2-Cre;Rosa26-lacZ mice, the lacZ-encoded B-galactosidase expression is specific to AMHR2+ cells and their progenies, and the B-galactosidase-positive cells represent the lineage of AMHR2 but do not stain for or correlate with the current expression of the receptor in these cells (39). Thus, we analyzed the general expression of AMHR2 in cells and tissues by Western blotting (Fig. 6). Human ovarian cancer cell lines are known to express high levels of AMHR2 and have been used as a positive indicator for AMH expression and function (40). All ovarian cancer cell lines, as well as primary human ovarian surface epithelial (HOSE) cells and the human fallopian tube epithelial (FTE) immortalized cell line, expressed AMHR2 (41) (Fig. 6*A*), which was not found human mammary fibroblasts. Only the OVSAHO ovarian cancer cell line, a presumptive model for high-grade serous ovarian carcinoma

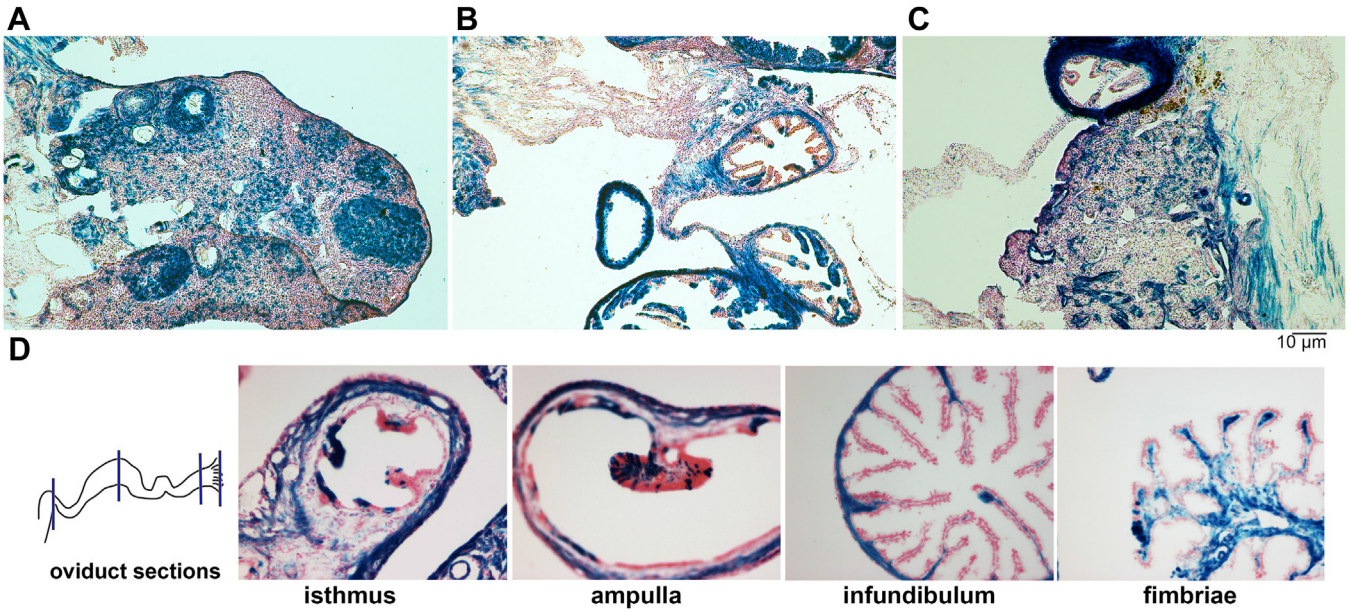

Figure 4. LacZ staining of AMHR2-Cre+;Rosa ± ovaries and oviducts. *A–B*, the ovarian surface of adult mice is mosaic for AMHR2-Cre+;Rosa ± epithelial cells, as shown by positive LacZ (blue X-Gal) staining. Granulosa cells of the ovarian follicles also stain positive for LacZ. *B*, epithelial areas of the oviduct are heterogeneous for LacZ staining. *C*, X-Gal staining of an AMHR2-Cre+;Rosa+/−;Wv/Wv ovary; note the intra-ovarian proliferation of epithelial lesions. *D*, Cross sections of the oviduct represent areas from the isthmus, ampulla, infundibulum, and fimbriae, from *left* to *right*, as indicated in the diagram.

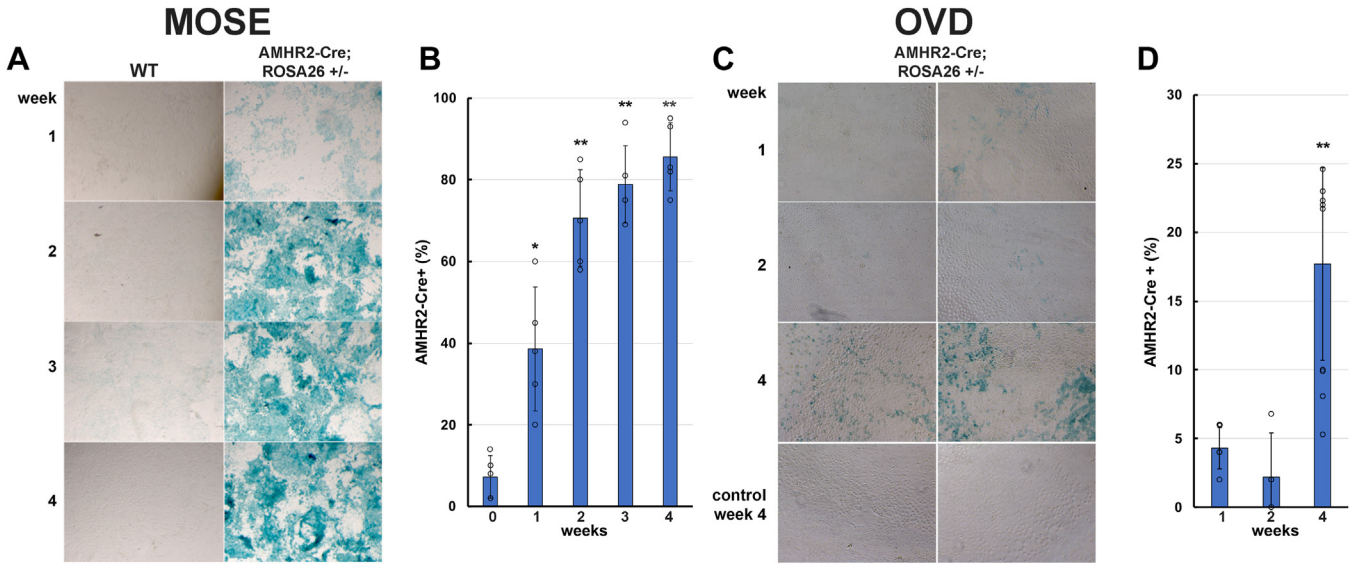

Figure 5. Expansion of AMHR2-Cre+;Rosa ± MOSE and OVD epithelial cells *in vitro*. *A–B*, primary cultures of MOSE and (C-D) OVD epithelial cells were established from 4-month-old AMHR2-Cre+;Rosa ± mice and allowed to expand in culture for 1 to 4 weeks. LacZ (X-Gal) staining of the cultures was performed. *B–D*, the percentage of X-Gal positive cells was calculated from an average of at least three separate fields, expressed as mean ± s.d. Significant difference from the starting time point was calculated for each subsequent time point using an unpaired two-tailed Student's *t* test, shown as $*p < 0.05$ and $**p = 0.0001$. Results are representative of three separate experiments. Images were taken at 63 × magnification.

(42), the most predominant form of ovarian cancer, did not express the predicted 63 kDa form. We saw variable expression in lysates from whole ovaries and oviducts, which might relate to the age of the animal. Whole tissue lysates from ovaries, oviducts, and uteri contain much less AMHR2 than male testes, as expected (Fig. 6*B*). The gonadal form of AMHR2 is typically slightly larger on SDS-PAGE than the adrenal gland isoform. Normal gonadal tissues and isolated oviduct and ovarian surface epithelial cells express AMHR2 and should be expected to respond to AMH.

AMH knockout mouse ovaries have aged but not proliferative phenotypes

AMH knockout mice were initially described as having an early loss of follicles, due to loss of AMH as a check to inhibit FSH-dependent cyclical recruitment of follicles and the transition from primordial to primary follicles (43), although AMH knockout mice have relatively normal lifetime reproductive capacity (44). We also observed in AMH knockout ovaries increased follicle maturation in young (1–2 months) and decreased numbers of primary follicles in mature (3–-7 months) ovaries (Fig. 7*A*). By 12 months, AMH knockout ovaries generally had a complete loss of follicles, compared to wild-type and AMH heterozygous ovaries that still contained multiple follicles and corpora lutea (Fig. 7*B*). Older AMH knockout ovaries showed a stromal-like pattern (recalling WvWv ovaries) and some epithelial proliferation on the ovarian surface (Fig. 7*C*), though they lack the highly proliferative epithelial layers that permeate throughout the ovaries as found for Wv/Wv mice, in which high gonadotropin levels do accelerate epithelial expansion (45). We also noted increased expansion of the ovarian bursa into surrounding fat and intraovarian cysts in the older AMH KO mice (Fig. 7*C*), as

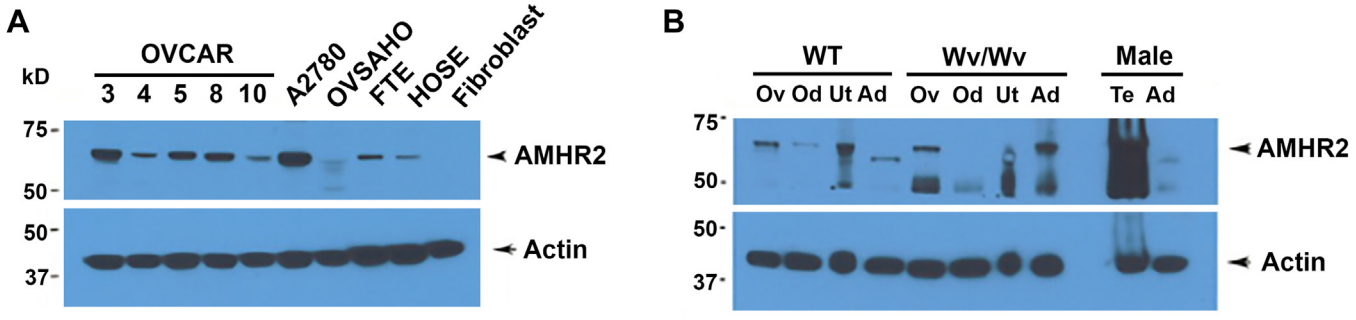

Figure 6. AMHR2 protein is expressed in ovarian cancer cells and primary cells and tissues. *A*, AMHR2 was detected in lysates from ovarian cancer cell lines (OVCAR-3, -4, -5, -8, -10; A2780; OVSAHO); an immortalized human fallopian tube cell line (FTE); and a primary cell culture obtained a human ovarian surface epithelium (HOSE). AMHR2 was not detected in a human mammary fibroblast culture. *B*, protein lysates were obtained from normal wild type (WT) and Wv/Wv (Wv) mouse ovaries (Ov), oviducts (Od), uteri (Ut), adrenal glands (Ad), and testes (Te). AMHR2 was detected using a mouse mAb (Abcam) at 1:2000 dilution and normalized to β-actin.

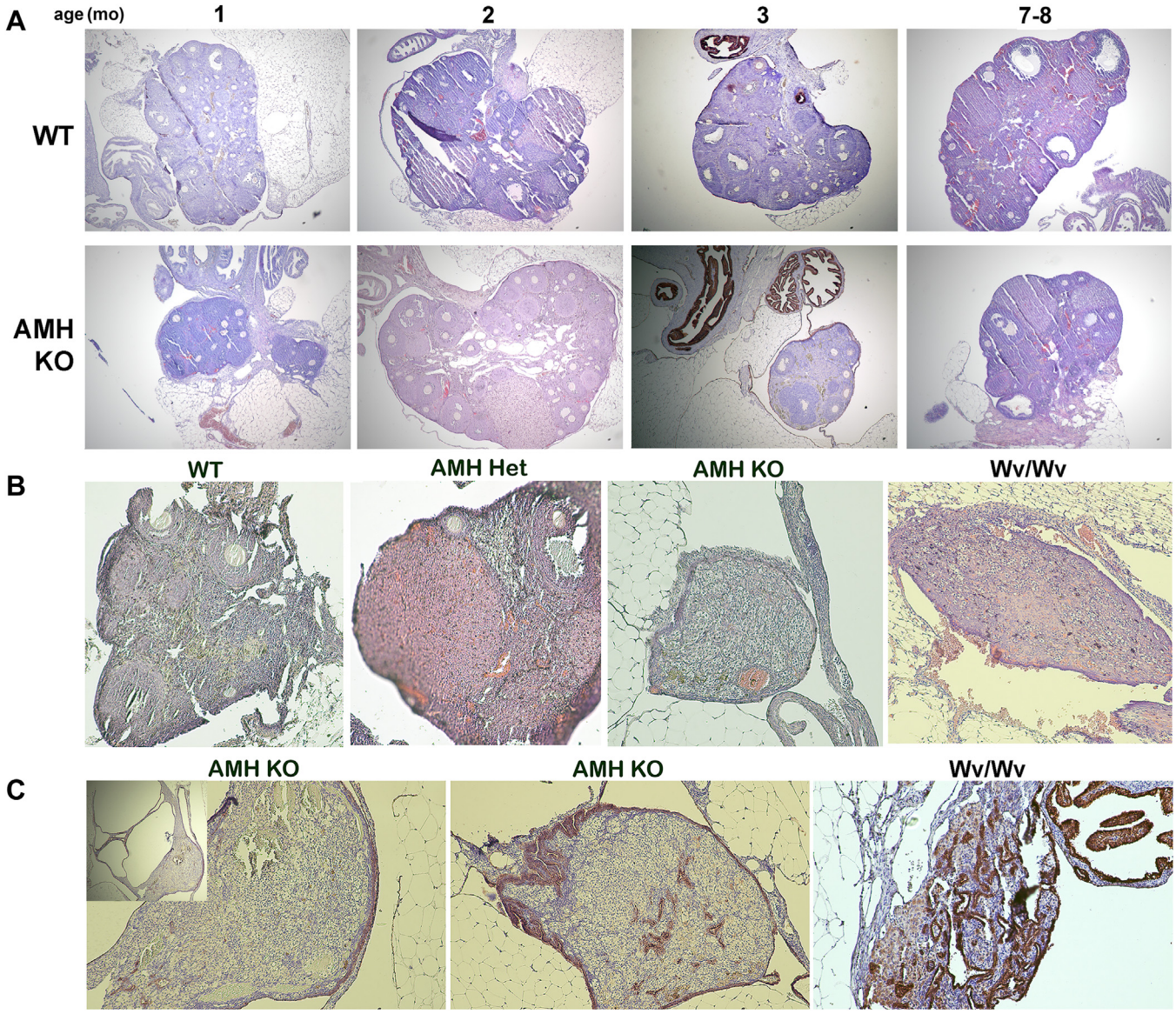

Figure 7. AMH knockout ovaries experience early aging and depletion of follicles. *A*, phenotypes of wild type and AMH knockout mouse ovaries at 1 to 8 months. Ovaries from 3-month-old mice were immunostained for epithelial cytokeratin 8 (arrows). Images were taken at 40 × final magnification. *B*, one-year-old mouse ovaries from WT, AMH heterozygous (AMH Het), AMH knockout (AMH KO), and Wv/Wv homozygous mice. *C*, example of ovarian cyst (inset showing the whole ovary at 40 × ; panel at 100 × magnification) and overt aging morphology in 1-year-old AMH KO ovaries, compared to a Wv/Wv ovary. Samples were immunostained for cytokeratin 8.

well as variable hyperplastic areas, although these changes did not appear consistently. These results suggest that ovarian follicle-secreted AMH does influence a subpopulation of ovarian surface epithelial cells that express the receptor AMHR2. AMH knockout mice also have a mild phenotype of ovarian surface epithelial proliferation and morphological changes, but overall have an ovarian phenotype much less severe than the early onset follicle-depleted WvWv mice, indicating that AMH is not the only factor involved in ovarian follicle-regulated epithelial growth.

Discussion

The current study was designed to analyze AMH as an ovarian follicle-derived factor in mediating the growth suppression of ovarian epithelial cells. Our *in vitro* analyses of cells isolated from control and mutant mice indicate that granulosa AMH is an active factor suppressing the growth of proliferating ovarian epithelial cells in culture. The results also suggest that AMHR2-positive epithelial cells found located within the ovarian surface and oviduct epithelia in a mosaic pattern is a stem/progenitor cell population that is responsible for the capacity for expansion of primary epithelial cells in culture. However, loss of AMH *in vivo* is insufficient to stimulate ramped proliferation of ovarian epithelia and the development of tubular adenomas as found in the Wv/Wv ovaries. Thus, we also conclude that additional ovarian follicle-derived factor(s) besides AMH also play roles in mediating the homeostasis of ovarian epithelia *in vivo*.

AMH pathway mediates stem cell-like properties in OSE cells

The *in vitro* co-culture and conditioned medium experiments, using cells isolated from wild-type and AMH (−/−) mice, showed that AMH is at least one predominant factor accounting for the suppressing activity of ovarian follicles or granulosa cells, as was demonstrated previously in neonatal ovaries from mice and rats, where AMH treatment inhibited proliferation of granulosa, surface epithelial, and stromal cells and inhibited granulosa cell differentiation (31). However, ovarian follicle depletion also leads to the loss of the feedback loop to the hypothalamus and a dramatic increase in the circulation LH and FSH produced by the pituitary (46). One possibility we consider is that the stimulation of LH and FSH, plus the loss of AMH, may account for the increased ovarian epithelial growth and tumor formation as a consequence of germ or ovarian follicle depletion, as proposed (Fig. 8).

The observation of a population of AMHR2-derived epithelial cells on the ovarian surface and oviduct epithelia prompts the speculation that these AMHR2-positive cells are epithelial progenitors or stem cells. During embryonic development and sex differentiation, female sex organs including the oviduct, uterine, and cervix develop from the Müllerian duct that expresses AMHR2 (22–24, 47, 48), whereas the ovary originates from mesodermal epithelium on the urogenital ridge (1), but both cell types share the common ancestor of the coelomic epithelium of the early embryo. In XY (male) embryos, the testis-determining gene SRY on the Y chromosome triggers testis development and the high expression and secretion of AMH (49). High AMH suppresses the development of AMHR2-positive Müllerian duct to develop into female organs. Thus, the AMHR2-positive cells can be considered stem/progenitor cells of the female organs, which are suppressed in male embryos that have high AMH. Indeed, the AMHR2-positive ovarian epithelial cells are considered to be the progenitor cancer stem cells (40, 49–53). It is generally thought that although the fallopian tube fimbriae is considered the source of high-grade ovarian cancer (54), some ovarian cancers may originate from the transformation of the AMHR2-positive epithelial cells on the ovarian surface (47).

Our study highlights clear differences in growth and expression properties between ovarian surface and oviduct

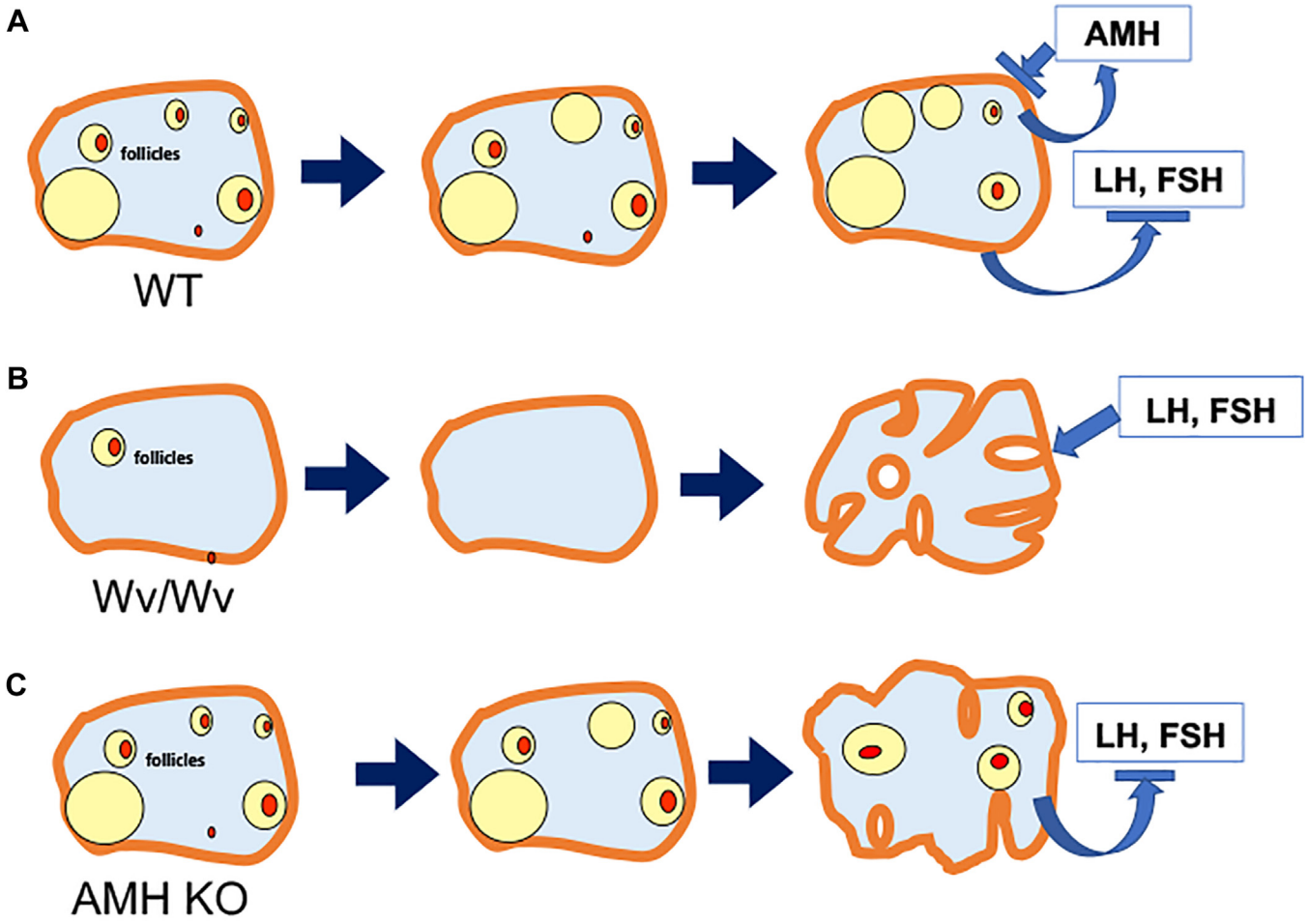

Figure 8. A decrease in AMH contributes to ovarian aging and proliferative potential of the surface epithelium. Scheme: *A*, in the normal cycling ovary, AMH produced by follicular granulosa cells can feed back and regulate growth of the epithelial cells on the surface and potentially nearby oviduct epithelial cells expressing AMHR2. The presence of follicles also provides feedback regulation of FSH and LH levels. *B*, in the WvWv mouse ovary, the absence of follicles results in the absence of AMH and unrestricted LH and FSH levels, conditions that permit epithelial expansion of the ovarian surface into the ovary. *C*, in AMH knockout mice, the lack of AMH leads to a more rapid decline in follicle numbers, but follicle-derived factors, such as progesterone and estrogen, are significant enough to regulate LH and FSH levels.

epithelial cells that correspond to recent single-cell RNA-sequencing (scRNA-seq) results and has implications for stem cell niches that contribute to their potential to develop into epithelial ovarian cancer (26). In conventional epithelial growth medium and conditions, MOSE cells proliferated robustly, and the AMHR2 lineage-derived OSE cells increased to dominate cultures over time. Likely AMHR2 marks stem-like cells, whose growth was promoted by culture conditions independently of AMH-AMHR2 signaling. These cells clearly expressed AMHR2 and were inhibited by both exogenous AMH and AMH present in granulosa cell-conditioned medium. By scRNA-seq, AMHR2-positive OSE populate the OSE stem cell niche that is largely independent of other accessory cell populations (26). Responsiveness of SMAD signaling to wild-type granulosa cell conditioned medium also corresponds to this stem-like population. In contrast, oviduct epithelial cells proliferated either slowly or inconsistently under the same growth conditions and were unresponsive to AMH-containing culture medium. These findings align with low or variable AMHR2 (LacZ+) expression, shown both in outgrowth cultures and in tissue sections from AMHR2-Cre;ROSA26 mice, as well as with published scRNA-seq data indicating that the majority of isolated fallopian tube epithelial cells may be quiescent/highly differentiated and lowly/slowly proliferative (26, 55). The fallopian tube epithelium (or oviduct in mice) is thought to be sustained by a non-epithelial stroma stem cell niche (26). These different expression programs, locations, and types of stem cell niches between ovarian surface and oviduct epithelial cells distinguish separate pathways to the development of ovarian cancers.

Moreover, AMHR2 has been reported expressed in 90% of primary epithelial ovarian cancers (EOCs), 78% of borderline malignancies, 77 to 86% of non-EOC ovarian tumors, and 56% of malignant ascites from grades III-IV ovarian cancers (40, 56–59), and these receptor-positive cancer cells are growth suppressed by MIS (50, 60), (40, 51, 53). Because of this expression, AMHR2 has been explored as a possible treatment option, and a human glyco-engineered monoclonal antibody to AMHR2 was developed, which was reported to have efficacy in pre-clinical studies (61). Yet, neither AMHR2 nor AMH expression is prognostic in ovarian cancer (https://www.proteinatlas.org/ENSG00000135409-AMHR2/pathology/ovarian+cancer), and AMHR2 is reported at a very low level in human oviduct epithelial cells (Fig. S3; +https://www.proteinatlas.org/ENSG00000135409-AMHR2/tissue/Fallopian+tube#rnaseq).

More recently, Chauvin *et al*. examined AMH and AMHR2 expression in human ovarian cancers in more detail (62), though their results differ somewhat from that of Protein Atlas. The authors analyzed the transcriptome profile of bulk RNA sequencing of primary human ovarian cancer cell lines and found by that AMH is expressed ubiquitously by primary ovarian cancer cells, whereas AMHR2 was not. AMHR2 expression was found in whole-tumor transcriptomes, as shown in Fig. S4. Instead, they found that AMHR2 was expressed in ovarian cancer-associated mesothelial cells and noted that genes of signaling pathways related to TGFβ superfamily were upregulated in the mesothelial cells. This finding aligns with our aggregate assessment of the Protein Atlas data that sees greater TGFβ expression related to ovarian cancer, as shown in Fig. S4. Obviously, since the expression of AMHR2 in EOC has been well documented, a greater understanding of AMHR2 expression, its location, and its mechanism is still required to know how to best use it as a potential therapeutic target.

The suppression of ovarian epithelial cells by ovarian-derived AMH may provide a mechanistic explanation for the etiology of some ovarian cancers, for which the risk is higher after menopause. Upon follicle depletion at menopause, one constraint of the microenvironment upon ovarian (and perhaps, to some limited degree, fallopian tube) epithelial cells is eliminated, allowing the growth and transformation of the epithelial cells to develop cancer (63). The germ cell-deficient Wv/Wv mice were used to model ovarian cancer risk at menopause (15). Our experimental results suggest that a lower AMH because of ovarian follicle depletion contributes to ovarian tumor development, but additional factors (such as LH and FSH and perhaps others) are also involved.

Experimental procedures

Animals

All mouse strains were maintained in the C57BL/6 background. Wild type (C57BL6/J) (JAX stock #000664), Wv (C57BL/6J-*Kit*$^{W\text{-}v}$/J) (Jax stock #000049), and AMH gene knockout (B6;129S7-Amhtm1Bhr/J) (JAX stock #002187) mice were obtained from Jackson Laboratory. The AMH-targeted mice were originally generated by replacing a 0.6 kb genomic fragment containing part of exon 1 and 2 with a neomycin selection cassette (22, 64). Matings between heterozygous mice (approximately 2–5 months of age) were set up to produce homozygous females. Mice were genotyped using the PCR protocol established by JAX lab protocol (Protocol Number 22677).

The founder pair of Misr2-Cre/Amhr2-Cre mice (strain B6; 129S7-*Amhr2*$^{tm3(cre)Bhr}$/MMnc) (http://www.mmrrc.org/strains/14245/014245.html) was obtained from the Mutant Mouse Regional Resource Centers (MMRRC) (58). The line contains an anti-Müllerian hormone type 2 receptor-targeted mutation by knock-in using the internal ribosome entry site (IRES)-Cre-pA FLP recombination target (FRT)-flanked pgk-neo-bpA cassette introduced into exon 5 of the Amhr2 locus and was originally generated in the lab of R. Behringer (65). The strains were in a 129/SvEvBrd X C57BL/6J mixed genetic background and were subsequently backcrossed to C57BL/6J mice. Generic Cre and LacZ primer sets were used to determine the genotype according to previously published protocols (20, 22). The ROSA26 Cre reporter mice for lineage tracing experiments were obtained from Jackson Laboratory (strain B6.129S4-*Gt(ROSA)26Sor*^{tm1Sor}/J) (66). The ROSA26 mice contain a loxP-flanked sequence of a stop codon that can be removed by the presence of Cre expression to activate LacZ.

All experiments using mice were performed in accordance with federal and state guidelines for the ethical and humane

use of laboratory animals, and the animal protocols were reviewed and approved by the University of Miami Institutional Animal Care and Use Committee.

Cell culture

Primary mouse ovarian surface epithelial (MOSE) cells were isolated from ovaries of wild-type C57BL/6 mice of 1 to 6 months of age by limited digestion in 0.25% Trypsin-EDTA solution (CellGro) at 37 °C for 20 to 30 min, as described previously (21, 67). Isolated MOSE cells were cultured in a well of a 6-well plate coated with 0.1% gelatin in DMEM containing 4% FBS (BenchMark FBS from Gemini), 1X insulin-transferrin-selenium (ITS) (Gemini), 1X non-essential amino acids (CellGro), and 1X antibiotic/antimycotic solution (Gemini), and expanded for 4 to 7 days, or in the presence of LIF and β-ME (68), and as indicated for specific experiments. To isolate oviduct epithelial cells, oviducts were cleared of fat, minced, and resuspended in chilled dissociation media (MEM containing 1.4 mg/ml Pronase and 0.1 mg/ml DNAse) and rocked at 4 °C for 48 h (25). Epithelial cells were obtained free of fibroblasts and blood cells that selectively stick to Primaria plates within 1 to 2 h, whereas the oviduct epithelial cells (OVD) do not. OVD cells were collected into a MOSE cell culture medium and grown on collagen-treated dishes. All cells were maintained at 37 °C in a humidified atmosphere of 5% CO_2.

Ovarian cancer cell lines were cultured in RMPI-1640 medium supplemented with 10% FBS and 1X penicillin/streptomycin (Gibco Life Technology). The OVCAR cells (3–5, 8, 10) were a generous gift of T. Hamilton's laboratory (Fox Chase Cancer Center, Philadelphia, PA). A2780 was purchased from ATCC (Manassas, VA). The FTE-3F human fallopian tube epithelial cell line was immortalized *via* double infection with a lentiviral dominant-negative TP53 vector and retroviruses with E7 and human telomerase (hTERT), as described (41), and were generously provided by Dr S. George, who also provided OVSAHO cells. Human ovarian surface epithelial cells and fibroblasts were isolated as described previously (69).

Cell growth was analyzed using a 3-(4,5-dimethyl-2-thiazolyl)-2,5-diphenyl-2H-tetrazolium bromide (MTT)-based WST-1 kit from Roche, which measures the conversion of the tetrazolium salt WST-1 into a soluble formazan dye. The production of dye correlates with the relative number of metabolically active cells in culture, detected as the absorbance at 450 nm on a standard plate reader. Relative cell numbers were measured in triplicate and are indicated as the mean ± standard deviation. Staining for LacZ in Amhr2-Cre +; ROSA26 ± cells and in cryosections of tissues followed standard protocols, using 1 mg/ml X-Gal (5-bromo-4-chloro-3-indolyl β-D-galactopyranoside) (from GoldBio) overnight at 37 °C (70).

Isolation of mouse ovarian granulosa cells

To isolate granulosa cells from mature follicles, immature 21-days mice were primed with 5 IU pregnant mare serum gonadotropins (PMSG) injected intraperitoneally, then 47 h later with 5 IU human chorionic growth hormone (hCG) (Sigma-Aldrich), according to standard protocols (27, 28). Ovaries were collected the following day. As a control, granulosa cells were also prepared from 21-days mice primed with diethylstilbestrol (DES) for three consecutive days. Diethylstilbestrol (DES) (from Sigma-Aldrich) was dissolved at a concentration of 10 mg/ml in sesame seed oil. The adult mice were injected subcutaneously using a 25-gauge needle (in the upper back) with 0.1 ml one time per day for 3 days (29). Ovaries were isolated free of the bursa and fat, and granulosa cells were released from follicles by puncturing the ovaries with a 25-gauge needle. Granulosa cells were expressed by gentle squeezing using the end of a sterile glass pipette bent into a "hockey stick" (as described by B. Vanderhyden, University of Ottawa, personal communication). Cells were collected into MOSE culture medium, washed, and plated at high density (approximately 5×10^5 cells/well) in a complete MOSE medium.

Co-culture of MOSE and granulosa cells

In a transwell system, MOSE cells were plated at 30,000 cells/well on gelatin-coated 24-well tissue culture dishes in 0.6 ml medium and incubated with wild-type granulosa cells grown on membrane filter inserts (Corning) at a density of 5×10^5 cells/filter/0.2 ml medium.

Immunodepletion of AMH from culture medium

Aliquots (50 μl) of a suspension (50% slurry) of magnetic Protein A/G beads (Pierce) were washed twice with PBS and rotated with 10 to 20 μl of anti-AMH rabbit polyclonal antibody (0.5 mg/ml stock, Abcam ab84952) or control Protein A/G and rabbit immunoglobins for 2 h at 4 °C, as described (71). This antibody was generated against a synthetic peptide corresponding to amino acids 468 to 517 of human AMH (NP_0000470). Bead-bound antibody was washed three times with cold PBS, then incubated with 500 μl of MOSE medium or granulosa cell-conditioned medium for 3 h at 4 °C. The supernatant was collected, centrifuged at 13,000 rpm for 15 min at 4 °C, and the resultant supernatant was used immediately in experiments or snap-frozen and stored at −80 °C for later use.

Immunoblotting and antibodies

Cells were plated in 12-well dishes and grown for 4 days before medium was replaced with MOSE medium containing LIF/β-ME, 0.2 μg/ml recombinant human TGFβ (BioLegend #580702), 0.5 μg/ml mouse EGF (Invitrogen #53003–018), or 6-days conditioned medium collected from wild type or AMH knockout granulosa cells. To prepare cell lysates, cells in monolayer culture were washed twice with cold PBS, immediately scraped, and collected in SDS sample buffer (BioRad #161–0737), then the lysates were boiled for 5 minutes. Protein samples were separated on 4 to 20% Tris/glycine gels (Invitrogen), electrotransferred to PDVF membranes, and immunoblotted with primary antibodies.

To prepare tissue lysates, organs were isolated free of fat, placed on ice, and washed 3X with ice-cold PBS, then minced

and homogenized in SDS sample buffer using a 2-mL Kontes tissue grind pestle on ice. Samples were separated and analyzed as described above.

The following antibodies were used: mouse monoclonal anti-actin (1:5000, Sigma-Aldrich, #A2228); rabbit polyclonal anti-ERK1/2 (1:1000, Cell Signaling Technology (CST), #9102); mouse monoclonal anti-Smad two-thirds (1:1000, BD Biosciences, #610843); rabbit polyclonal anti-phospho-Smad2 (Ser465/467) (1:1000, CST, #3101); rabbit polyclonal anti-phospho-ERK1/2 (1:000, CST, #9101); anti-rabbit polyclonal AMHR2 (1:1000, Invitrogen, PA5-93030), and anti-mouse monoclonal AMHR2 (1:100–1:1000, Abcam, ab64762). HRP-conjugated secondary antibodies were from BioRad and used as determined empirically at 1:5000-1:20,000 dilution. Clarity Western ECL substrate (BioRad, #1705060) was used to visualize the immunoblots.

Immunohistochemistry and X-Gal staining

For standard immunohistochemistry, ovarian horns, oviducts, and ovaries were collected, fixed overnight in 10% buffered formalin, and embedded in paraffin. Sections were sliced from blocks at 5 to 7 μm, attached to positively charged glass slides, and processed for immunohistochemistry as described previously (15, 17, 21). The rat Troma-1 anti-cytokeratin 8 antibody (AB_531826) was used at 1:500 dilution; TROMA-I was deposited to the Developmental Studies Hybridoma Bank by Brulet, P./Kemler, R. (DSHB Hybridoma Product TROMA-I). For Lac-Z staining of AMHR2-cre/ROSA26 reporter mice, tissues were fixed for 40 min in 4% paraformaldehyde on ice, soaked overnight in 30% sucrose at 4 °C, then embedded in OCT, and snap frozen and stored at −80 °C. All samples were sectioned into 15 μm slices using a Leica CM1860 cryostat at −20 °C. Tissue sections were processed for LacZ staining using X-Gal overnight at 37 °C as described (20).

Statistical analysis

The Student's unpaired two-tailed t test calculator offered online from GraphPad was used to compare and test for significance between two groups, where $p < 0.05$ is considered statistically significant. Results are plotted as mean of technical replicate samples ± standard deviation (sd), unless indicated otherwise. One way ANOVA analysis, which tests if the difference between the averages of two or more groups is significant, confirmed the data significance and was calculated using Statistics Kingdom ANOVA calculator (https://www.statskingdom.com/180Anova1way.html). Figures were plotted using Microsoft Excel and assembled using Microsoft Photoshop, or plotted using R software.

Data availability

All supporting data are included within the manuscript.

Supporting information—This article contains supporting information.

Acknowledgments—We are grateful for discussions, advice, assistance, and use of equipment from our colleagues—Sophia George, PhD; Zhengying Wang, PhD; Robert Moore, PhD; Valery Chavez, PhD; Josie Eid, MD; and Barbara Vanderhyden, PhD.

Author contributions—I. R. L. X. software; I. R. L. X., E. R. S., and D. Y. formal analysis; I. R. L. X., S. L., E. R. S., and D. Y. data curation; X-x X. and E. R. S. writing–original draft; X-x X. and E. R. S. supervision; X-x X. resources; X-x X. project administration; X-x X., S. L., E. R. S., and D. Y. methodology; X-x X. and E. R. S. funding acquisition; X-x X. and E. R. S. conceptualization; S. L. and D. Y. investigation; E. R. S. writing–review & editing.

Funding and additional information—The research was supported by funds from the University of Miami Dean's NIH Bridge Award UM and University of Miami SEEDS Leadership Award (ERS), NICHD R03HD071244 (ERS), CDMRP DoD Concept Awards BC097189 and BC076832 (XXX), and NCI grants R01 CA230916, R01 CA095071, R01 CA099471, and CA79716 (XXX). The content is solely the responsibility of the authors and does not necessarily represent the official views of the National Institutes of Health.

Conflict of interest—The authors declare that they have no conflicts of interest with the contents of this article.

Abbreviations—The abbreviations used are: AMH/MIS, Anti-Müllerian Hormone/Müllerian Inhibitory Substance; AMHR2, AMH receptor 2; MOSE, mouse ovarian surface epithelial.

References

1. Hummitzsch, K., Anderson, R. A., Wilhelm, D., Wu, J., Telfer, E. E., Russell, D. L., *et al.* (2015) Stem cells, progenitor cells, and lineage decisions in the ovary. *Endocr. Rev.* **36**, 65–91
2. Lorenzo, H. K., Teixeira, J., Pahlavan, N., Laurich, V. M., Donahoe, P. K., and MacLaughlin, D. T. (2002) New approaches for high-yield purification of Müllerian inhibiting substance improve its bioactivity. *J. Chromatogr. B Analyt Technol. Biomed. Life Sci.* **766**, 89–98
3. Eppig, J. J. (2018) Reproduction: oocytes call, granulosa cells connect. *Curr. Biol.* **28**, R354–R356
4. Schulz, B. O., Krebs, D., Diedrich, K., Knoll, H., Hobbel, K., and Hamerich, U. (1985) Effects of granulosa cells and gonadotrophins on maturation of rabbit oocytes in vitro. *Arch. Gynecol.* **236**, 135–143
5. Matzuk, M. M., Burns, K. H., Viveiros, M. M., and Eppig, J. J. (2002) Intercellular communication in the mammalian ovary: oocytes carry the conversation. *Science* **296**, 2178–2180
6. Skinner, M. K., Schmidt, M., Savenkova, M. I., Sadler-Riggleman, I., and Nilsson, E. E. (2008) Regulation of granulosa and theca cell transcriptomes during ovarian antral follicle. *Development Mol. Reprod. Dev.* **75**, 1457–1472
7. Gamwell, L. F., Collins, O., and Vanderhyden, B. C. (2012) The mouse ovarian surface epithelium contains a population of LY6A (SCA-1) expressing progenitor cells that are regulated by ovulation-associated factors. *Biol. Reprod.* **87**, 80
8. Lu, J. K., Anzalone, C. R., and LaPolt, P. S. (1994) Relation of neuroendocrine function to reproductive decline during aging in the female rat. *Neurobiol. Aging* **15**, 541–544
9. Camaioni, A., Ucci, M. A., Campagnolo, L., De Felici, M., and Klinger, F. G. (2022) The process of ovarian aging: it is not just about oocytes and granulosa cells. *J. Assist Reprod. Genet.* **39**, 783–792
10. Mara, J. N., Zhou, L. T., Larmore, M., Johnson, B., Ayiku, R., Amargant, F., *et al.* (2020) Ovulation and ovarian wound healing are impaired with advanced reproductive age. *Aging (Albany NY)* **12**, 9686–9713
11. Nicosia, S. V. (1987) The aging ovary. *Med. Clin. North Am.* **71**, 1–9

12. Mintz, B., and Russell, E. S. (1957) Gene-induced embryological modifications of primordial germ cells in the mouse. *J. Exp. Zool* **134**, 207–237
13. Nocka, K., Tan, J. C., Chiu, E., Chu, T. Y., Ray, P., Traktman, P., *et al.* (1990) Molecular bases of dominant negative and loss of function mutations at the murine c-kit/white spotting locus: W37, Wv. *W41 W EMBO J.* **9**, 1805–1813
14. Reith, A. D., Rottapel, R., Giddens, E., Brady, C., Forrester, L., and Bernstein, A. (1990) W mutant mice with mild or severe developmental defects contain distinct point mutations in the kinase domain of the c-kit receptor. *Genes Dev.* **4**, 390–400
15. Smith, E. R., Yeasky, T., Wei, J. Q., Miki, R. A., Cai, K. Q., Smedberg, J. L., *et al.* (2012) White spotting variant mouse as an experimental model for ovarian aging and menopausal biology. *Menopause* **19**, 588–596
16. Murphy, E. D. (1972) Hyperplastic and early neoplastic changes in the ovaries of mice after genic deletion of germ cells. *J. Natl. Cancer Inst.* **48**, 1283–1295
17. Yang, W. L., Cai, K. Q., Smedberg, J. L., Smith, E. R., Klein-Szanto, A., Hamilton, T. C., *et al.* (2007) A reduction of cyclooxygenase 2 gene dosage counters the ovarian morphological aging and tumor phenotype in Wv mice. *Am. J. Pathol.* **170**, 1325–1336
18. Cai, K. Q., Wang, Y., Smith, E. R., Smedberg, J. L., Yang, D. H., Yang, W. L., *et al.* (2015) Global deletion of Trp53 reverts ovarian tumor phenotype of the germ cell-deficient white spotting variant (Wv) mice. *Neoplasia* **17**, 89–100
19. Smith, E. R., Yang, W. L., Yeasky, T., Smedberg, J., Cai, K. Q., and Xu, X. X. (2013) Cyclooxygenase-1 inhibition prolongs postnatal ovarian follicle lifespan in mice. *Biol. Reprod.* **89**, 103
20. Arango, N. A., Kobayashi, A., Wang, Y., Jamin, S. P., Lee, H. H., Orvis, G. D., *et al.* (2008) A mesenchymal perspective of Mullerian duct differentiation and regression in Amhr2-lacZ mice. *Mol. Reprod. Dev.* **75**, 1154–1162
21. Wang, Y., Cai, K. Q., Smith, E. R., Yeasky, T. M., Moore, R., Ganjei-Azar, P., *et al.* (2016) Follicle depletion provides a permissive environment for ovarian. *Carcinogenesis Mol. Cell Biol.* **36**, 2418–2430
22. Jamin, S. P., Arango, N. A., Mishina, Y., Hanks, M. C., and Behringer, R. R. (2003) Genetic studies of the AMH/MIS signaling pathway for Mullerian duct regression. *Mol. Cell Endocrinol* **211**, 15–19
23. Kobayashi, A., and Behringer, R. R. (2003) Developmental genetics of the female reproductive tract in mammals. *Nat. Rev. Genet.* **4**, 969–980
24. Orvis, G. D., and Behringer, R. R. (2007) Cellular mechanisms of Müllerian duct formation in the mouse. *Dev. Biol.* **306**, 493–504
25. Fotheringham, S., Levanon, K., and Drapkin, R. (2011) Ex vivo culture of primary human fallopian tube epithelial cells. *J. Vis. Exp.* https://doi.org/10.3791/2728
26. Qin, G., Park, E. S., Chen, X., Han, S., Xiang, D., Ren, F., *et al.* (2023) Distinct niche structures and intrinsic programs of fallopian tube and ovarian surface epithelial cells. *iScience* **26**, 105861
27. Vanderhyden, B. C., and Armstrong, D. T. (1990) Effects of gonadotropins and granulosa cell secretions on the maturation and fertilization of rat oocytes in vitro. *Mol. Reprod. Dev.* **26**, 337–346
28. Emori, C., and Sugiura, K. (2014) Role of oocyte-derived paracrine factors in follicular. *Development Anim. Sci. J.* **85**, 627–633
29. Chakravorty, A., Mahesh, V. B., and Mills, T. M. (1991) Regulation of follicular development by diethylstilboestrol in ovaries of immature rats. *J. Reprod. Fertil.* **92**, 307–321
30. Andersen, C. Y., Schmidt, K. T., Kristensen, S. G., Rosendahl, M., Byskov, A. G., and Ernst, E. (2010) Concentrations of AMH and inhibin-B in relation to follicular diameter in normal human small antral follicles. *Hum. Reprod.* **25**, 1282–1287
31. Meinsohn, M. C., Saatcioglu, H. D., Wei, L., Li, Y., Horn, H., Chauvin, M., *et al.* (2021) Single-cell sequencing reveals suppressive transcriptional programs regulated by MIS/AMH in neonatal ovaries. *Proc. Natl. Acad. Sci. U. S. A.* **118**, e2100920118
32. Howard, J. A., Hart, K. N., and Thompson, T. B. (2022) Molecular mechanisms of AMH signaling. *Front. Endocrinol. (Lausanne)* **13**, 927824
33. di Clemente, N., Jamin, S. P., Lugovskoy, A., Carmillo, P., Ehrenfels, C., Picard, J. Y., *et al.* (2010) Processing of anti-mullerian hormone regulates receptor activation by a mechanism distinct from TGF-beta. *Mol. Endocrinol.* **24**, 2193–2206
34. Sengle, G., Ono, R. N., Lyons, K. M., Bachinger, H. P., and Sakai, L. Y. (2008) A new model for growth factor activation: type II receptors compete with the prodomain for BMP-7. *J. Mol. Biol.* **381**, 1025–1039
35. Ragin, R. C., Donahoe, P. K., Kenneally, M. K., Ahmad, M. F., and MacLaughlin, D. T. (1992) Human Müllerian inhibiting substance: enhanced purification imparts biochemical stability and restores antiproliferative effects. *Protein Expr. Purif.* **3**, 236–245
36. Donahoe, P. K., Clarke, T., Teixeira, J., Maheswaran, S., and MacLaughlin, D. T. (2003) Enhanced purification and production of Müllerian inhibiting substance for therapeutic applications. *Mol. Cell Endocrinol* **211**, 37–42
37. Josso, N., and Picard, J. Y. (2022) Genetics of anti-Mullerian hormone and its signaling pathway. *Best Pract. Res. Clin. Endocrinol. Metab.* **36**, 101634
38. Dimri, G. P., Lee, X., Basile, G., Acosta, M., Scott, G., Roskelley, C., *et al.* (1995) A biomarker that identifies senescent human cells in culture and in aging skin *in vivo*. *Proc. Natl. Acad. Sci. U. S. A.* **92**, 9363–9367
39. Ghosh, A., Syed, S. M., Kumar, M., Carpenter, T. J., Teixeira, J. M., Houairia, N., *et al.* (2020) In vivo cell fate tracing provides No evidence for mesenchymal to epithelial transition in adult fallopian tube and uterus. *Cell Rep* **31**, 107631
40. Masiakos, P. T., MacLaughlin, D. T., Maheswaran, S., Teixeira, J., Fuller, A. F., Jr., Shah, P. C., *et al.* (1999) Human ovarian cancer, cell lines, and primary ascites cells express the human Mullerian inhibiting substance (MIS) type II receptor, bind, and are responsive to MIS. *Clin. Cancer Res.* **5**, 3488–3499
41. George, S. H., Milea, A., Sowamber, R., Chehade, R., Tone, A., and Shaw, P. A. (2016) Loss of LKB1 and p53 synergizes to alter fallopian tube epithelial phenotype and high-grade serous tumorigenesis. *Oncogene* **35**, 59–68
42. Domcke, S., Sinha, R., Levine, D. A., Sander, C., and Schultz, N. (2013) Evaluating cell lines as tumour models by comparison of genomic profiles. *Nat. Commun.* **4**, 2126
43. Durlinger, A. L., Kramer, P., Karels, B., de Jong, F. H., Uilenbroek, J. T., Grootegoed, J. A., *et al.* (1999) Control of primordial follicle recruitment by anti-Mullerian hormone in the mouse ovary. *Endocrinology* **140**, 5789–5796
44. Guo, R., and Pankhurst, M. W. (2020) Accelerated ovarian reserve depletion in female anti-Mullerian hormone knockout mice has no effect on lifetime fertilitydagger. *Biol. Reprod.* **102**, 915–922
45. Murphy, E. D., and Beamer, W. G. (1973) Plasma gonadotropin levels during early stages of ovarian tumorigenesis in mice of the W x -W u genotype. *Cancer Res.* **33**, 721–723
46. Lobo, R. A., Kelsey, J. L., and Marcus, R. (2000) *Menopause: Biology and Pathobiology*, Academic Press, San Diego, CA
47. Broer, S. L., Broekmans, F. J., Laven, J. S., and Fauser, B. C. (2014) Anti-Müllerian hormone: ovarian reserve testing and its potential clinical implications. *Hum. Reprod. Update* **20**, 688–701
48. MacLaughlin, D. T., and Donahoe, P. K. (2004) Sex determination and differentiation. *N. Engl. J. Med.* **350**, 367–378
49. Josso, N., Lamarre, I., Picard, J.-Y., Berta, P., Davies, N., Morichon, N., *et al.* (1993) Anti-Müllerian hormone in early. *Hum. Dev. Early Hum. Dev.* **33**, 91–99
50. Kim, J. H., MacLaughlin, D. T., and Donahoe, P. K. (2014) Müllerian inhibiting substance/anti-Müllerian hormone: a novel treatment for gynecologic tumors. *Obstet. Gynecol. Sci.* **57**, 343–357
51. Pieretti-Vanmarcke, R., Donahoe, P. K., Pearsall, L. A., Dinulescu, D. M., Connolly, D. C., Halpern, E. F., *et al.* (2006) Mullerian Inhibiting Substance enhances subclinical doses of chemotherapeutic agents to inhibit human and mouse ovarian cancer. *Proc. Natl. Acad. Sci. U. S. A.* **103**, 17426–17431
52. Connolly, D. C., Bao, R., Nikitin, A. Y., Stephens, K. C., Poole, T. W., Hua, X., *et al.* (2003) Female mice chimeric for expression of the simian virus 40 TAg under control of the MISIIR promoter develop epithelial ovarian cancer. *Cancer Res.* **63**, 1389–1397
53. Szotek, P. P., Pieretti-Vanmarcke, R., Masiakos, P. T., Dinulescu, D. M., Connolly, D., Foster, R., *et al.* (2006) Ovarian cancer side population defines cells with stem cell-like characteristics and Mullerian Inhibiting

Substance responsiveness. *Proc. Natl. Acad. Sci. U. S. A.* **103**, 11154–11159
54. Labidi-Galy, S. I., Papp, E., Hallberg, D., Niknafs, N., Adleff, V., Noe, M., *et al.* (2017) High grade serous ovarian carcinomas originate in the fallopian tube. *Nat. Commun.* **8**, 1093
55. Dinh, H. Q., Lin, X., Abbasi, F., Nameki, R., Haro, M., Olingy, C. E., *et al.* (2021) Single-cell transcriptomics identifies gene expression networks driving differentiation and tumorigenesis in the human fallopian tube. *Cell Rep.* **35**, 108978
56. Song, J. Y., Chen, K. Y., Kim, S. Y., Kim, M. R., Ryu, K. S., Cha, J. H., *et al.* (2009) The expression of Mullerian inhibiting substance/anti-Mullerian hormone type II receptor protein and mRNA in benign, borderline and malignant ovarian neoplasia. *Int. J. Oncol.* **34**, 1583–1591
57. Sakalar, C., Mazumder, S., Johnson, J. M., Altuntas, C. Z., Jaini, R., Aguilar, R., *et al.* (2015) Regulation of murine ovarian epithelial carcinoma by vaccination against the cytoplasmic domain of anti-mullerian hormone receptor II. *J. Immunol. Res.* **2015**, 630287
58. Bakkum-Gamez, J. N., Aletti, G., Lewis, K. A., Keeney, G. L., Thomas, B. M., Navarro-Teulon, I., *et al.* (2008) Mullerian inhibiting substance type II receptor (MISIIR): a novel, tissue-specific target expressed by gynecologic cancers. *Gynecol. Oncol.* **108**, 141–148
59. Mazumder, S., Swank, V., Komar, A. A., Johnson, J. M., and Tuohy, V. K. (2020) Immunotherapy of ovarian cancer with a monoclonal antibody specific for the extracellular domain of anti-Mullerian hormone receptor II. *Oncotarget* **11**, 1894–1910
60. Basal, E., Ayeni, T., Zhang, Q., Langstraat, C., Donahoe, P. K., Pepin, D., *et al.* (2016) Patterns of mullerian inhibiting substance type II and candidate type I receptors in epithelial ovarian cancer curr. *Mol. Med.* **16**, 222–231
61. Bougherara, H., Nemati, F., Nicolas, A., Massonnet, G., Pugniere, M., Ngo, C., *et al.* (2017) The humanized anti-human AMHRII mAb 3C23K exerts an anti-tumor activity against human ovarian cancer through tumor-associated macrophages. *Oncotarget* **8**, 99950–99965
62. Chauvin, M., Meinsohn, M. C., Dasari, S., May, P., Iyer, S., Nguyen, N. M. P., *et al.* (2023) Cancer-associated mesothelial cells are regulated by the anti-Mullerian hormone axis. *Cell Rep* **42**, 112730
63. Smith, E. R., and Xu, X. X. (2008) Ovarian ageing, follicle depletion, and cancer: a hypothesis for the aetiology of epithelial ovarian cancer involving follicle depletion. *Lancet Oncol.* **9**, 1108–1111
64. Behringer, R. R., Finegold, M. J., and Cate, R. L. (1994) Mullerian-inhibiting substance function during mammalian sexual development. *Cell* **79**, 415–425
65. Jamin, S. P., Arango, N. A., Mishina, Y., Hanks, M. C., and Behringer, R. R. (2002) Requirement of Bmpr1a for Müllerian duct regression during male sexual development. *Nat. Genet.* **32**, 408–410
66. Soriano, P. (1999) Generalized lacZ expression with the ROSA26 Cre reporter strain. *Nat. Genet.* **21**, 70–71
67. Capo-Chichi, C. D., Yeasky, T. M., Smith, E. R., and Xu, X. X. (2016) Nuclear envelope structural defect underlies the main cause of aneuploidy in ovarian carcinogenesis BMC. *Cell Biol* **17**, 37
68. Flesken-Nikitin, A., Hwang, C. I., Cheng, C. Y., Michurina, T. V., Enikolopov, G., and Nikitin, A. Y. (2013) Ovarian surface epithelium at the junction area contains a cancer-prone stem cell niche. *Nature* **495**, 241–245
69. Smith, E. R., Cai, K. Q., Smedberg, J. L., Ribeiro, M. M., Rula, M. E., Slater, C., *et al.* (2010) Nuclear entry of activated MAPK is restricted in primary ovarian and mammary epithelial cells. *PLoS One* **5**, e9295
70. Nagy, A., Gertsenstein, M., Vintersten, K., and Behringer, R. (2007) Staining frozen mouse embryo sections for β-galactosidase (lacZ) activity. *Cold Spring Harbor Protoc.* **2007**, pdb.prot4726
71. Kwon, Y. W., Heo, S. C., Jeong, G. O., Yoon, J. W., Mo, W. M., Lee, M. J., *et al.* (2013) Tumor necrosis factor-alpha-activated mesenchymal stem cells promote endothelial progenitor cell homing and angiogenesis. *Biochim. Biophys. Acta* **1832**, 2136–2144